FEATURE ARTICLE

Neural Dynamics and the Fundamental Mechanisms of Event-related Brain Potentials

Ankoor S. Shah[1,2], Steven L. Bressler[3], Kevin H. Knuth[4], Mingzhou Ding[3], Ashesh D. Mehta[5], Istvan Ulbert[6] and Charles E. Schroeder[1,2]

[1]Department of Neuroscience, Albert Einstein College of Medicine, Bronx, NY 10461, USA, [2]Cognitive Neuroscience and Schizophrenia Program, Nathan Kline Institute, Orangeburg, NY 10962, USA, [3]Center for Complex Systems and Brain Sciences, Florida Atlantic University, Boca Raton, FL 33431, USA, [4]Computational Sciences Division, Code IC, NASA Ames Research Center, Moffett Field, CA 94035-1000, USA, [5]Department of Neurological Surgery, Weill Medical College of Cornell University, New York, NY 10021, USA and [6]Institute for Psychology, Hungarian Academy of Sciences, Budapest, H-1394, Hungary

Event-related potentials (ERPs) provide a critical link between the hemodynamic response, as measured by functional magnetic resonance imaging, and the dynamics of the underlying neuronal activity. Single-trial ERP recordings capture the oscillatory activity that are hypothesized to underlie both communication between brain regions and amplified processing of behaviorally relevant stimuli. However, precise interpretations of ERPs are precluded by uncertainty about their neural mechanisms. One influential theory holds that averaged sensory ERPs are generated by partial phase resetting of ongoing electroencephalographic oscillations, while another states that ERPs result from stimulus-evoked neural responses. We formulated critical predictions of each theory and tested these using direct, intracortical analyses of neural activity in monkeys. Our findings support a predominant role for stimulus-evoked activity in sensory ERP generation, and they outline both logic and methodology necessary for differentiating evoked and phase resetting contributions to cognitive and motor ERPs in future studies.

Keywords: current source density (CSD), evoked response, phase resetting, oscillatory activity, single-trial analyses, synchronization

Introduction

For nearly 30 years, two opposing theories about the neural origins of sensory event-related potentials (ERPs) have been debated. The theory that has dominated the discussion recently states that the sensory stimulus induces 'phase resetting' of ongoing electroencephalographic (EEG) rhythms in each trial and that averaging these phase-coherent rhythms produces the ERP (Sayers *et al.*, 1974; Makeig *et al.*, 2002; Jansen *et al.*, 2003). The alternative view states that the stimulus 'evokes' an additive, neural-population response in each trial and that averaging these evoked responses produces the ERP (Jervis *et al.*, 1983; Hillyard *et al.*, 1985; Hillyard and Picton, 1987; Vaughan and Arezzo, 1988; Mangun, 1992; Schroeder *et al.*, 1995). Resolving this debate has become crucial with the advent of functional magnetic resonance imaging (fMRI) because ERPs provide a critical link between the hemodynamic response indexed by fMRI and the temporal dynamics of underlying neuronal activity (Murray *et al.*, 2002). Equally important, a growing body of literature shows interactions between event-related neural responses indexed by the ERP and ongoing brain oscillations (Brandt *et al.*, 1991; Mast and Victor, 1991; Fries *et al.*, 2001a; Liang *et al.*, 2002), which are hypothesized to underlie communication between brain areas (Gray *et al.*, 1989) and to amplify the sensory processing of behaviorally relevant stimuli (Fries *et al.*, 2001b).

Earlier attempts at defining the neural mechanisms of the ERP were limited by two factors: (i) scalp ERPs are indirect measures, recorded at a distance from their neural sources, and (ii) the critical predictions of each model were not clearly delineated. Here we address both limitations. First, we detail several 'critical' predictions of each model (Table 1) that are amenable to empirical testing. Secondly, we report the direct evaluation of each requirement by analysis of single-trial, intracortical activity in awake, behaving monkeys.

Materials and Methods

Subjects and Task

Data for these analyses were collected from two male macaques performing a visual oddball discrimination paradigm. The Institutional Animal Care and Use Committee at the Nathan Kline Institute approved all experimental procedures. Subjects were presented with random streams of 'standard' and 'oddball' stimuli with standards presented during 86% of the trials and oddballs presented during 14% of the trials. The monkey pressed a switch to initiate stimulus presentation and held it until he detected an oddball. Appropriate release of the switch earned a drop of juice. The standard visual stimulus was a 10 μs, red-light flash presented on a diffusing screen subtending 12 retinal degrees and centered on a fixation point. The deviant stimulus differed slightly in intensity or color. Data analyses concerned only the neural responses to the standard, non-target stimulus. An infrared eye tracker monitored eye position, and stimuli were presented only when fixation was within a 1° window around the fixation point. Each experimental session consisted of between 474 and 3007 (mean = 1430.5 and median = 1443) presentations of the standard visual stimulus. Both of these monkeys also served in selective attention studies not covered by the present report. Further details are available in Mehta *et al.* (2000a).

Table 1
Predictions of the phase resetting and evoked models of ERP generation at the dominant frequency of the ERP

	Property	Phase resetting model	Evoked model
1	Ongoing EEG oscillations prior to stimulus onset	yes	no requirement
2	Stimulus-induced phase concentration	yes	likely
3	Stimulus-induced increase in signal power	no[a]	yes

[a]See Theoretical Predictions for the nuances of this point.

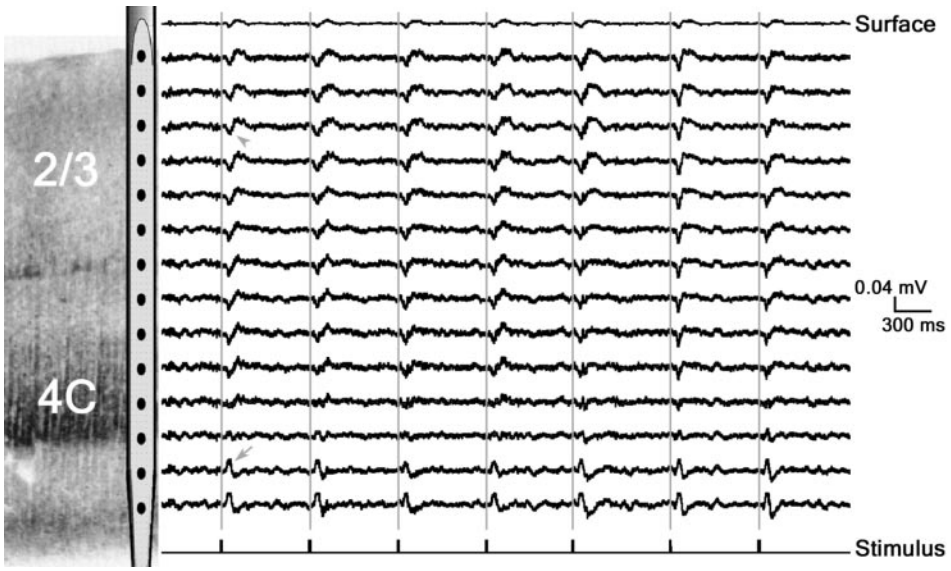

Figure 1. Field potential activity recorded from a multielectrode positioned in area V1 shows very little pre-stimulus oscillatory activity (data from experimental session VA2). A schematic of the multielectrode positioning in V1 is illustrated on the left, and potentials from an occipital surface electrode (top trace) and from all fourteen intracranial channels are shown on the right. The vertical ticks on the bottom trace denote presentation of the red-light stimulus. A prominent surface-negative potential reflects the local stimulus-related response, which undergoes polarity inversion across Layer 4 (see arrowhead and arrow) (Givre *et al.*, 1994; Schroeder *et al.*, 1998). Pre-stimulus activity appears quite small in comparison to the stimulus-related activity.

Data Collection

An experimental session began with positioning a linear-array multielectrode in either V1 or posterior IT such that the contact array was perpendicular to the layering of the area (Fig. 1, left). A detailed description of these methods can be found in Schroeder *et al.* (1998) (Schroeder *et al.*, 1998). In one session, two multielectrodes arrays were inserted intracranially to record simultaneously from sites in V1 and IT. In all cases, electrode contacts had an impedance between 0.1 and 0.3 MΩ and were spaced at equal intervals. Intercontact spacing was either 150 or 200 μm, depending on the particular multielectrode used during that session. Neuroelectric signals were amplified with a pass band of 3–3000 Hz, digitized at 2000 Hz using a PC-based data acquisition system (Neuroscan, El Paso, TX), and analyzed using custom-made code in MATLAB (The Mathworks Inc., Natick, MA).

Data Analyses

Data from each session were prepared for analyses by first epoching the EEG from –300 to 300 ms, with zero denoting the onset of stimulus presentation. Secondly, the average CSD profile was computed, and the laminar positioning of each CSD channel was defined as either supragranular, granular, or infragranular according to the typical (averaged) CSD profile of that cortical area (Schroeder *et al.*, 1998). Thirdly, the full-wave rectified, average CSD signal for each supragranular and granular channel was integrated, and the two channels (one in each layer) with the largest integral areas were chosen for analyses. Fourth, the post-stimulus average CSD (defined as the average CSD waveform from 0 to 300 ms) in these two channels was multiplied by a Hamming window, and the discrete Fourier transform (DFT) of the resultant was calculated. The dominant frequency of the ERP (see Table 2) in each layer was defined as the frequency bin with the greatest power in this spectrum. Fifth, single-trial CSD signals in both chosen channels were split into pre- and post-stimulus signals, multiplied by a Hamming window, and converted to the frequency domain by a 600-point DFT yielding pre- and post-stimulus, single-trial frequency spectra. With a sampling frequency of 2000 Hz and a 600-sample DFT, the frequency bins were 3.33 Hz in width and encompassed 0 to 1000 Hz.

Single-trial power and phase distributions at the dominant frequency (i.e. the frequency bin chosen in step 4 above) were taken from the single-trial spectra calculated in step 5. The Wilcoxon Signed-Rank test was used to compare pre- and post-stimulus power distributions. Phase distributions were evaluated using a modified Kuiper V statistic, which when >2.00 indicates that the distribution departs from uniformity with a significance probability of 0.01 (Fisher, 1996). Also, sample circular variance was calculated for the phase data because these values represent a circular population (Fisher, 1996).

Single-trial total power distributions for the pre- and post-stimulus periods were calculated as the integral of the single-trial, power spectra from 0 to 1000 Hz. For each experimental session, these distributions were normalized so that the median post-stimulus total power equalled 1.0 $(mV/mm^2)^2$. The distributions for the supragranular tissue are displayed as box plots (see Fig. 6*b*,*c*). The lower and upper lines of the 'box' bound the 25th and 75th percentiles of the distribution, and the middle line represents the median of that sample. The position of the median line with respect to the upper and lower lines indicates the skew of the distribution. Notches in the box around the median indicate the confidence interval about that median. Vertical

Table 2
Dominant frequency (in Hz) of the granular and supragranular current source density signals that were chosen for analysis in each experimental session

Area	Session	Dominant frequency	
		Supragranular (Hz)	Granular (Hz)
V1	VA2	3.33	6.67
	V66	6.67	3.33
	R47	3.33	6.67
	R69	6.67	6.67
IT	V71	3.33	3.33
	VE7	3.33	3.33
	RAO	6.67	13.33
	R37	3.33	10.00

lines above and below the box show the extent of the data, minus outliers.

Results

Theoretical Predictions

Strict interpretations of the phase resetting and evoked models pose differing predictions for three specific properties of single-trial field potentials, as outlined in Table 1. Phase resetting makes three main predictions. Under property 1, it predicts that activity at the dominant frequency of the ERP must be present in the pre-stimulus period. Under property 2, phase resetting predicts that the transition between the pre- to the post-stimulus periods must involve phase concentration (i.e. synchronization of an EEG rhythm across trials) (Sayers *et al.*, 1974; Makeig *et al.*, 2002; Jansen *et al.*, 2003). These two predictions are actually critical requirements for the operation of phase resetting. On the other hand, the evoked model is tolerant of a wide range of pre-stimulus activity, and it predicts phase concentration because an evoked, single-trial response is relatively phase-locked to stimulus onset. Regarding property 3, a strict version of the phase resetting model predicts (requires) that the pre- to post-stimulus transition must occur without increase in power at the dominant frequency of the ERP. The evoked model, in contrast, requires a post-stimulus increase in power at that frequency. It is important to emphasize that the phase resetting model does not deny that evoked activity occurs. Rather it assumes that the evoked responses occur outside the dominant frequency of the ERP and serve as a trigger for resetting the phase of the local EEG oscillations. What the strict phase resetting model does hold is that in averaging over numerous trials, phase-reset EEG rhythms form the substrate for the ERP rather than the local evoked responses. Thus increase in EEG power at the dominant frequency of the ERP can rule out an exclusive account in terms of phase resetting.

Direct Empirical Analysis

Our analysis considered cortical areas at both low and high levels of visual processing, namely primary visual cortex (area V1) and inferotemporal (IT) cortex. This allowed us to test the possibility that the evoked model may account for ERP generation in cortical areas closer to the receptor surface (retina), while the phase resetting model may describe ERP contributions from areas more removed from the retina and increasingly influenced by 'state' variables such as attention (Maunsell and Newsome, 1987; Mehta *et al.*, 2000a; Fries *et al.*, 2001b). Data were collected from two male macaque monkeys while they performed a task requiring discrimination between target and non-target visual stimuli. In each experimental session, a linear-array multielectrode with 14 equally spaced contacts was inserted acutely into V1 and/or IT such that the array spanned all layers of that area at an angle perpendicular to the laminae (Fig. 1, left). Local field potentials were sampled, and a second-derivative approximation of the current source density (CSD) was computed (Freeman and Nicholson, 1975; Schroeder *et al.*, 1995). Quantitative analyses (presented below) utilized the CSD measure instead of the field potential because the CSD approximation eliminates activity generated outside the cortical area of interest, which may contaminate local field potential recordings. Moreover, the CSD profile directly addresses the electrogenesis of ERPs, because it is an index of the transmembrane current flow patterns responsible for generating the local field potential. The local multiunit action potential (MUA) profile was sampled from the same electrode contacts to provide an independent link between the ERP and neuronal activity. In each animal, two V1 and two IT recordings were analyzed for a total of four sessions in each area.

Qualitative Properties

Qualitative properties of the raw data from V1 support the Evoked Model over Phase Resetting. Figure 1 illustrates field potentials recorded from V1 of one subject during presentation of non-target stimuli. A concurrent EEG recording from an electrode over the occipital brain surface near the recording site is shown (top trace) along with recordings from all fourteen contacts of the multielectrode array. A prominent single-trial, stimulus-evoked response is observed as a negative field potential above layer 4, which inverts to a positive potential below layer 4 (arrowhead and arrow in Fig. 1), indicating that it is locally generated (Schroeder *et al.*, 1995). However, the pre-stimulus activity is relatively small and displays no apparent oscillations at the frequency of the evoked response. Since previous studies show that the generator for this potential lies in the layer 4C (Schroeder *et al.*, 1992, 1995, 1998), we examined the data from that layer across all trials. Figure 2 depicts the concomitant single-trial ERPs (field potentials), multi-unit activities (MUA) and transmembrane current flow densities (CSD). Relatively few pre-stimulus oscillations are observed across trials, and the post-stimulus period shows a discrete field potential negativity, which, accompanied by a burst of MUA and a current sink in the CSD, indicates net local excitation. When viewed at this scale, the obvious event-related responses appear to support the evoked model, and the lack of comparable pre-stimulus oscillations discount the phase resetting model.

Although these data exhibit few pre-stimulus EEG oscillations and crisp event-related responses, these aspects vary across experimental sessions. For simplicity, all analyses described henceforth focus on neural signals from one electrode contact in supragranular (layer 2/3) tissue and one in granular (layer 4) tissue. Previous studies indicate that these two laminar divisions contain major generators of the average surface ERPs (Schroeder *et al.*, 1992, 1995, 1998). Figure 3 depicts simultaneous field potential recordings from multielectrodes in V1 and IT during a different experimental session (VE7). Although the single-trial, evoked response is still apparent in V1 (arrow), both recordings display more obvious pre-stimulus oscillations than those in recorded in session VA2 (see Figures 1 and 2). Comparison of concurrent V1 and IT recordings underscores a further point that generalizes across all experimental sessions: the ratio of pre- to post-stimulus oscillatory activity is larger in higher-order area IT than in primary visual area V1 (see Quantitative Analyses).

Quantitative Analyses

Quantitative analyses were performed to evaluate properties 1–3 of Table 1. To evaluate property 1, we computed the median ratio of pre- to post-stimulus power at the dominant frequency of the ERP across all trials, experimental sessions, and subjects. For the supragranular layer recordings, this ratio increased from 0.13 $(mV/mm^2)^2$ in V1 to 0.27 $(mV/mm^2)^2$ in IT. The corresponding comparison for the granular layer showed

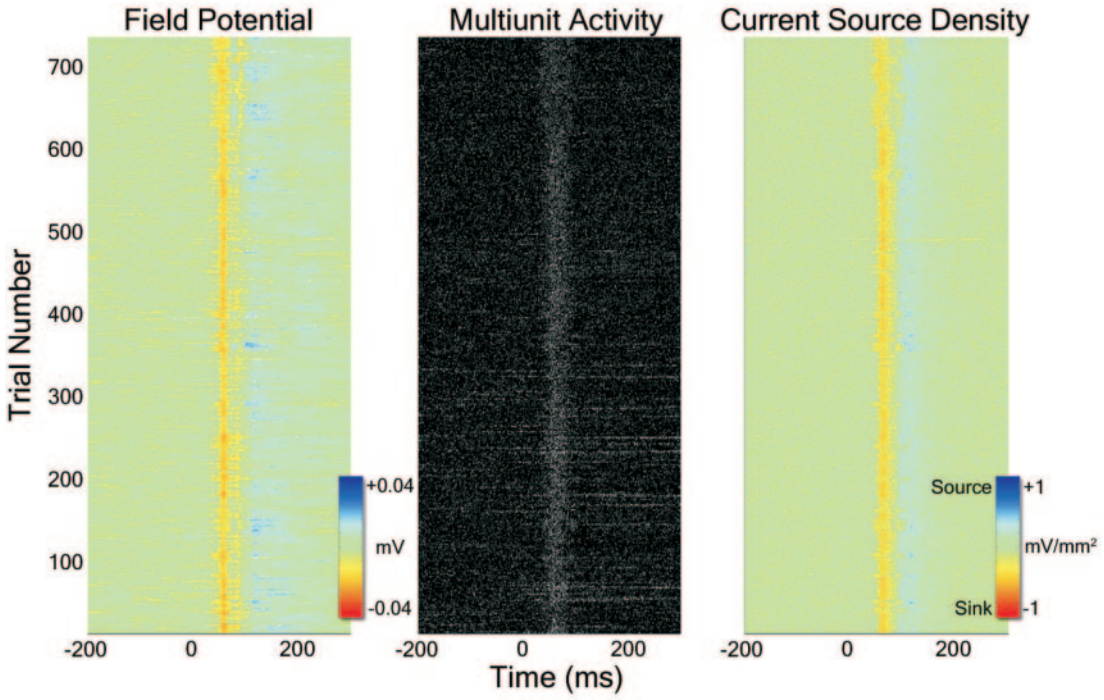

Figure 2. Field potential, multiunit activity, and current-source density (CSD) from an electrode channel located in the granular layer across all trials of the V1 session presented in Figure 1. The pre-stimulus periods have little activity when compared with the post-stimulus periods.

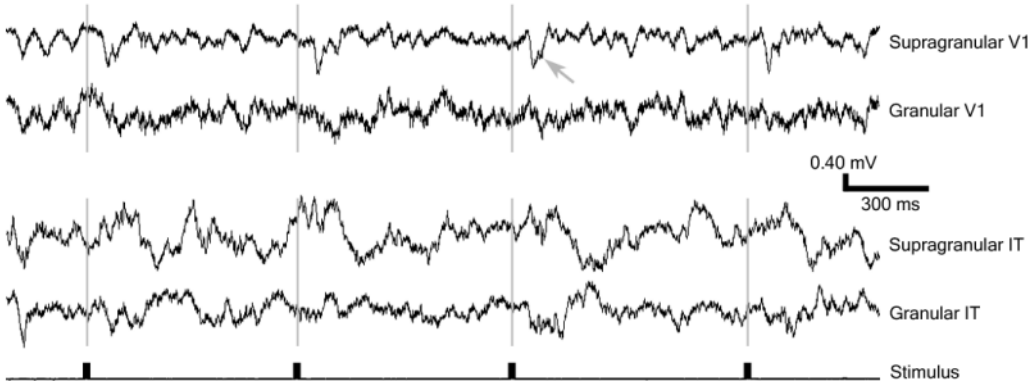

Figure 3. Simultaneous field potential recordings from V1 and IT (experimental session VE7). Pre-stimulus activity in each area displays prominent ongoing oscillations. The single-trial, event-related response is still visible in V1 (arrow) but more difficult to observe in IT. Despite the presence of these pre-stimulus rhythms, the total power in IT still demonstrates a pre- to post-stimulus increase (see Fig. 6*c*, session VE7). For simplicity, only recordings from two sites in each cortical area are illustrated. The vertical ticks in the bottom trace denote presentation of the red-light flash.

an increase from 0.20 $(mV/mm^2)^2$ in V1 to 0.37 $(mV/mm^2)^2$ in IT. The V1 to IT differences in both layers were significant (Wilcoxon rank-sum test, $P < 0.01$). These results indicate two important properties. First, both cortical areas have some pre-stimulus activity at the dominant frequency, which is required for the phase resetting model and consistent with the evoked model under property 1. Second, the pre-stimulus power in IT is significantly greater than that in V1, suggesting that IT may be more prone to phase resetting, and hence the mechanisms of ERP generation may differ across levels of the hierarchy.

Property 2 specifies model-relevant changes in the phase of oscillatory activity, and so we compared pre- and post-stimulus phase distributions at the dominant frequency of the ERP (in our case, the dominant frequency of the averaged, post-stimulus CSD in each electrode contact considered for each session). Examples from supragranular V1 and IT are shown in Figure 4. Pre-stimulus activity at the dominant frequency should yield a uniform phase distribution because stimulus presentation, which defines the pre-stimulus period, occurred at random interstimulus intervals. Across sessions and layers, the majority (13/16) of pre-stimulus phase distributions did not differ from uniformity, while all post-stimulus distributions were statistically different from uniformity (modified Kuiper V statistic, $P < 0.01$) (Fisher, 1996). In all cases, the pre- to post-stimulus transition demonstrated a drastic decrease in circular variance suggesting stimulus-induced phase concentration. The phase resetting model requires this result, but the finding is also compatible with the evoked model; therefore, the observation of phase concentration does not differentiate between the models. In fact, further analyses (see property 3 results

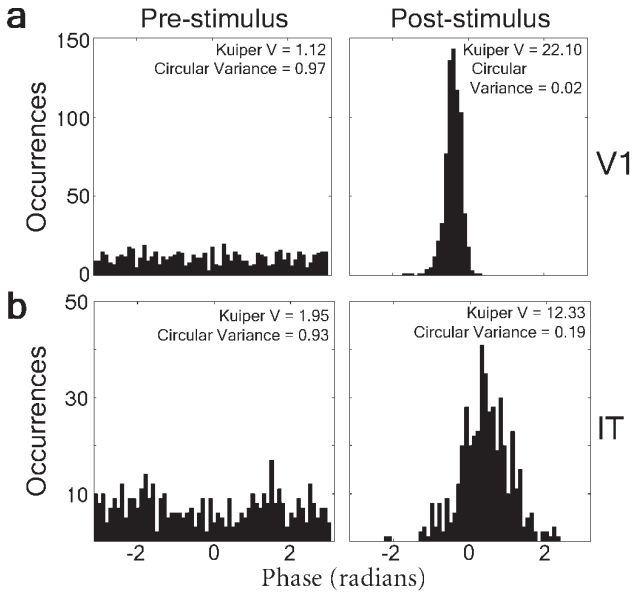

Figure 4. Stimulus-induced phase modulation during V1 session VA2 and IT session V71. Pre-stimulus phase distributions at the dominant frequency of the ERP across trials in supragranular V1 (*a*) and IT (*b*) cannot be statistically differentiated from uniformity (modified Kuiper V statistic < 2.0 indicates $P < 0.01$). Post-stimulus distributions, on the other hand, show a departure from uniformity ($P < 0.01$) and illustrate phase concentration, as evidenced by the decrease in circular variance.

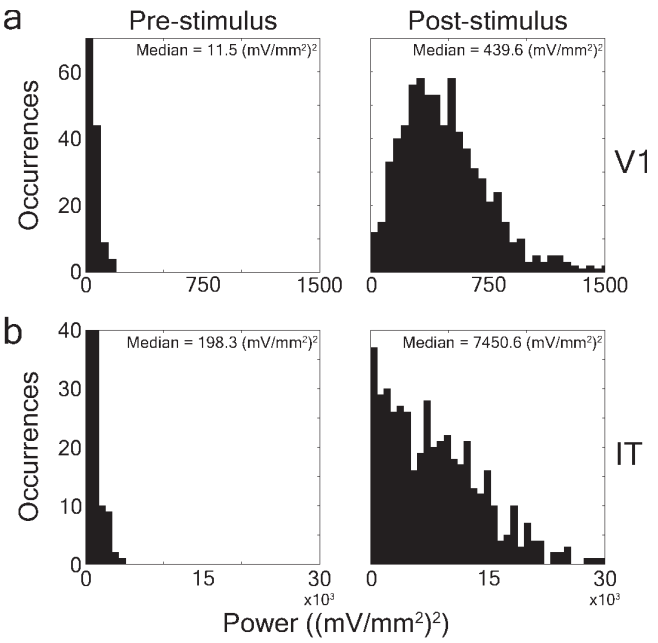

Figure 5. Stimulus-induced power modulation during V1 session VA2 and IT session V71. Power distributions at the dominant frequency across trials in supragranular V1 (*a*) and IT (*b*) demonstrate significant increases during the pre- to post-stimulus transition (Wilcoxon signed-rank test, $P < 0.01$).

below) suggest that the majority of the effect is likely caused by addition of relatively phase-locked power at the dominant frequency of the ERP.

While properties 1 and 2 fail to differentiate between the phase resetting and evoked models, property 3 generates opposing predictions that are readily testable. The phase resetting model requires no addition of stimulus-induced power at the dominant frequency of the ERP, while this is a necessity for the evoked model. Across the entire data set irrespective of cortical layer or area, we found a significant increase in median power (Wilcoxon signed-rank test, $P < 0.01$) and variance from the pre- to the post-stimulus periods at the dominant frequency. Figure 5 illustrates this stimulus-induced power modulation in the supragranular layers of V1 and IT. Similar results were found for the granular layer. This power increase satisfies the prediction of property 3 for the evoked model and violates it for the phase resetting model.

We performed two control analyses to detect any errors caused by confining the above quantification to the dominant frequency of the ERP. First, we examined the single-trial power at every frequency between 0 and 1000 Hz in the granular and supragranular data to see if phase resetting may be operating at a different frequency. At all frequencies, the median post-stimulus power was significantly greater than the median pre-stimulus power across all layers and areas (Wilcoxon signed-rank test, $P < 0.01$ with Bonferroni correction). Examples of median spectra from supragranular V1 are shown in Figure 6*a*. Note that new peaks are observed at ~23 and 40 Hz in the post-stimulus spectrum, indicating stimulus-induced addition of new frequency components. Given these results, we also expected a pre- to post-stimulus increase in total power. As illustrated in Figure 6*b*,*c* for the supragranular layers of V1 and IT, respectively, all experiments displayed significant increases in the median total power (Wilcoxon signed-rank test, $P <$ 0.01). Parallel findings were noted for the granular layers. These results suggest an overall increase in neural activity across frequency bands: a finding compatible with the evoked model and incompatible with the phase resetting model.

As a second control, we examined key qualities of the pre-stimulus spectrum to see if it resembled the post-stimulus spectrum as might be expected if phase resetting generated the ERP. First, as illustrated in Figure 6*a*, we found that the peak frequency of the pre-stimulus period most often differed from the dominant frequency of the ERP (three of four recordings in supragranular V1, two of four recordings in granular V1, three of four recordings in supragranular IT, and three of four recordings in granular IT). Additionally, the half-maximal bandwidth about the peak frequency of the pre-stimulus spectrum was wider than that around the dominant frequency of the post-stimulus spectrum. Fourteen of 16 recordings showed this effect, while one showed no change (supragranular V1 in session R69) and one showed an increase (supragranular IT in session V71) in half-maximal bandwidth. The shift in peak frequency and the stimulus-induced sharpening of power about the dominant frequency strongly indicate that the pre-stimulus activity has a fundamentally different organization than the post-stimulus activity, which again argues against the phase resetting model as the mechanism underlying ERPs.

Discussion

Earlier studies from our laboratory showed that, at least for averaged visual ERPs, components recorded at the brain surface or scalp resulted from the summation of contributions from different cortical and subcortical areas (Schroeder *et al.*, 1991, 1992, 1995; Givre *et al.*, 1994; Mehta *et al.*, 2000a,b). The remarkable correspondence between the intracortical ERP profile in V1 and the ERP at the overlying brain surface (Fig. 1) illustrates the fidelity of this relationship on a trial-by-trial basis.

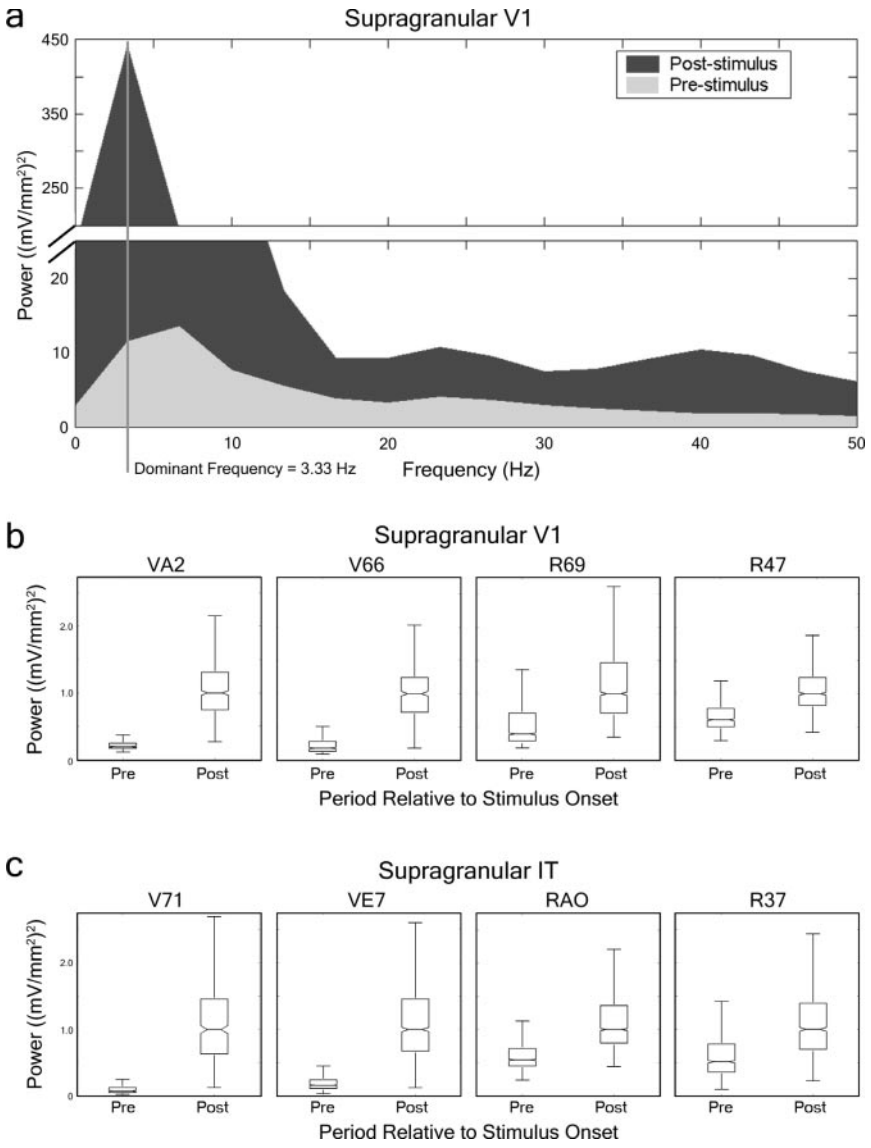

Figure 6. Signal power across frequencies during the pre- and post-stimulus periods. (*a*) Median pre- and post-stimulus power spectra for the supragranular CSD in V1 session VA2 display a stimulus-induced increase in power across frequencies (Wilcoxon signed-rank test, $P < 0.01$ with Bonferroni correction). Note that the peaks at ~23 and ~40 Hz in the post-stimulus spectrum denote the addition of new frequency components and that a shift in the dominant frequency occurs between the pre- and post-stimulus periods. (*b, c*) The distributions of normalized power in the supragranular V1 (*b*) and IT (*c*) for each experimental session are displayed graphically as box plots (see Data Analyses). Each pair represents a different experimental session in subject 'V' or 'R'.

Moreover, a recent study from another laboratory reveals a definitive stimulus-induced increase in signal power in macaque V1 and V4 (Rols *et al.*, 2001), which suggests an evoked contribution to the scalp ERP according to the present framework. The present results, based on single trial analyses, show a clear increase in EEG power accompanied with phase concentration at the dominant frequency of the ERP regardless of the power in the pre-stimulus period. This clearly rules out the possibility that Phase Resetting alone could account for ERP generation.

Penny *et al.* (2002) proposed amplitude and phase modulation as possible mechanisms for ERP generation, and they likened these processes to the evoked and phase resetting models, respectively. Our data demonstrate empirically that amplitude and phase modulation both operate in neocortex. However, it is also obvious that phase modulation (concentration) will be detected in single-trial analyses even when a strict evoked mechanism is operating. That is, transmembrane currents triggered by stochastic firing of the inputs to local neurons and by random non-synaptic currents will generate the baseline EEG. Thus, pre-stimulus activity will contain power in the frequency bands of the ERP, and these frequency components will likely have uniform phase distributions because the generating events are random. When a stimulus is presented, the evoked response will be produced, and it will be relatively phase-locked to stimulus presentation. Phase modulation in the form of concentration will be observed simply because there is random pre-stimulus activity in frequency bands of the ERP and a relatively phase-locked post-stimulus response.

It is noteworthy that under the present conceptual framework, the evoked model can incorporate most of the major observations cited as support for phase resetting. For example, although the widely reported interactions between EEG oscilla-

tions and the ERP (Brandt *et al.*, 1991; Mast and Victor, 1991; Fries *et al.*, 2001a,b; Liang *et al.*, 2002; Makeig *et al.*, 2002) are required by phase resetting, these observations also fit with the evoked model as there is no restriction on pre-stimulus activity influencing evoked responses. More specifically, ERP enhancement during trials in which pre-stimulus activity is large (Brandt *et al.*, 1991; Liang *et al.*, 2002; Makeig *et al.*, 2002) may result because ongoing rhythms and evoked responses are generated by overlapping components of the same biophysical machinery. Any modulation of either would tend to affect both processes in a yoked fashion.

While the present results clearly support a predominant role for evoked responses in generating sensory event-related potentials, they leave open the possibility that phase resetting contributes to this process. The fact that pre-stimulus oscillations show a systematic increase in power from V1 to IT suggests the possibility of a shift from a mainly evoked mechanism at low levels of sensory processing to a mechanism more influenced by phase resetting at higher processing levels. Further, phase resetting may play an important role in cortical feedback-mediated ERP components such as the 'selection negativity', which is observed in the comparison between attended and non-attended, non-target stimuli in selective attention experiments (Harter *et al.*, 1982; Hillyard, 1985; Mehta *et al.*, 2000a,b). Finally, phase resetting may operate by default in the generation of ERPs that have no defined sensory 'evoking' stimulus, such as the 'missing stimulus P3' (Simson *et al.*, 1977; Michalewski *et al.*, 1982) and motor potentials associated with self-paced movements (Arezzo *et al.*, 1987). Although further experiments will be required to address these questions, the conceptual framework outlined in the present study identifies conditions necessary for phase resetting to contribute to ERPs (properties 1 and 2) as well as conditions under which its contributions can be ruled out (property 3).

Notes

We thank Tammy McGinnis, Noelle O'Connell, and Robert Lindsley for technical support. We also thank Drs. Olivier Bertrand, Robert Desimone, Steve Hillyard, Gyorgy Karmos, and Peter Lakatos for numerous discussions and suggestions during the preparation of this manuscript. The National Institute on Mental Health (MH60358 and MH64204), Medical Scientist Training Program (T32M07288), National Science Foundation (IBN0090717), NASA IDU/IS/CICT Program and NASA Aerospace Technology Enterprise supported this work. Data in this paper are from a thesis to be submitted in partial fulfilment of the requirements for a D.Phil. at the Graduate Division of Medical Sciences, Albert Einstein College of Medicine.

Address correspondence to Charles E. Schroeder, PhD, 140 Old Orangeburg Road, Orangeburg, NY 10962, USA. Email: schrod@nki.rfmh.org.

References

Arezzo JC, Tenke CE, Vaughan HG Jr (1987) Movement-related potentials within the hippocampal formation of the monkey. Brain Res 401:79–86.

Brandt ME, Jansen BH, Carbonari JP (1991) Pre-stimulus spectral EEG patterns and the visual evoked response. Electroencephalogr Clin Neurophysiol 80:16–20.

Fisher NI (1996) Statistical analysis of circular data. Cambridge: Cambridge University Press.

Freeman JA, Nicholson C (1975) Experimental optimization of current source density technique for anuran cerebellum. J Neurophysiol 38:369–382.

Fries P, Neuenschwander S, Engel AK, Goebel R, Singer W (2001a) Rapid feature selective neuronal synchronization through correlated latency shifting. Nat Neurosci 4:194–200.

Fries P, Reynolds JH, Rorie AE, Desimone R (2001b) Modulation of oscillatory neuronal synchronization by selective visual attention. Science 291:1560–1563.

Givre SJ, Schroeder CE, Arezzo JC (1994) Contribution of extrastriate area V4 to the surface-recorded flash VEP in the awake macaque. Vision Res 34:415–438.

Gray CM, Konig P, Engel AK, Singer W (1989) Oscillatory responses in cat visual cortex exhibit inter-columnar synchronization which reflects global stimulus properties. Nature 338:334–337.

Harter MR, Aine C, Schroeder CE (1982) Hemispheric differences in the neural processing of stimulus location and type: effects of selective attention on visual evoked potentials. Neuropsychologia 20:421–438.

Hillyard SA (1985) Electrophysiology of human selective attention. Trends Neurosci 8:400–405.

Hillyard SA, Picton TW (1987) Electrophysiology of cognition. In: Handbook of physiology. Section 1. The nervous system (Plum F, ed.), vol. 5, pp. 519–584. Oxford: Oxford University Press.

Hillyard SA, Munte TF, Neville HJ (1985) Visual–spatial attention, orienting and brain physiology. In: Attention and performance. XI. Mechanisms of attention (Posner MI, Marin OS, eds), pp. 63–84. Hillsdale, NJ: Erlbaum.

Jansen BH, Agarwal G, Hegde A, Boutros NN (2003) Phase synchronization of the ongoing EEG and auditory EP generation. Clin Neurophysiol 114:79–85.

Jervis BW, Nichols MJ, Johnson TE, Allen E, Hudson NR (1983) A fundamental investigation of the composition of auditory evoked potentials. IEEE Trans Biomed Eng 30:43–50.

Liang H, Bressler SL, Ding M, Truccolo WA, Nakamura R (2002) Synchronized activity in prefrontal cortex during anticipation of visuomotor processing. Neuroreport 13:2011–2015.

Makeig S, Westerfield M, Jung TP, Enghoff S, Townsend J, Courchesne E, Sejnowski TJ (2002) Dynamic brain sources of visual evoked responses. Science 295:690–694.

Mangun GR (1992) Human brain potentials evoked by visual stimuli: induced rhythms or time-locked components? In: Induced rhythms in the brain (Basar E, Bullock TH, eds), pp. 217–231. Boston, MA: Birkhauser.

Mast J, Victor JD (1991) Fluctuations of steady-state VEPs: interaction of driven evoked potentials and the EEG. Electroencephalogr Clin Neurophysiol 78:389–401.

Maunsell JH, Newsome WT (1987) Visual processing in monkey extrastriate cortex. Annu Rev Neurosci 10:363–401.

Mehta AD, Ulbert I, Schroeder CE (2000a) Intermodal selective attention in monkeys. I: Distribution and timing of effects across visual areas. Cereb Cortex 10:343–358.

Mehta AD, Ulbert I, Schroeder CE (2000b) Intermodal selective attention in monkeys. II: Physiological mechanisms of modulation. Cereb Cortex 10:359–370.

Michalewski HJ, Patterson JV, Bowman TE, Litzleman DK, Thompson LW (1982) A comparison of the emitted late positive potential in older and young adults. J Gerontol 37:52–58.

Murray MM, Wylie GR, Higgins BA, Javitt DC, Schroeder CE, Foxe JJ (2002) The spatiotemporal dynamics of illusory contour processing: combined high-density electrical mapping, source analysis, and functional magnetic resonance imaging. J Neurosci 22:5055–5073.

Penny WD, Kiebel SJ, Kilner JM, Rugg MD (2002) Event-related brain dynamics. Trends Neurosci 25:387–389.

Rols G, Tallon-Baudry C, Girard P, Bertrand O, Bullier J (2001) Cortical mapping of gamma oscillations in areas V1 and V4 of the macaque monkey. Vis Neurosci 18:527–540.

Sayers BM, Beagley HA, Henshall WR (1974) The mechansim of auditory evoked EEG responses. Nature 247:481–483.

Schroeder CE, Tenke CE, Givre SJ, Arezzo JC, Vaughan HGJ (1991) Striate cortical contribution to the surface-recorded pattern-reversal VEP in the alert monkey. Vision Res 31:1143–1157. [Erratum appears in Vision Res 31(11):I.]

Schroeder CE, Tenke CE, Givre SJ (1992) Subcortical contributions to the surface-recorded flash-VEP in the awake macaque. Electroencephalogr Clin Neurophysiol 84:219–231.

Schroeder CE, Steinschneider M, Javitt DC, Tenke CE, Givre SJ, Mehta AD, Arezzo JC, Vaughan HGJ (1995) Localization of ERP generators and identification of underlying neural processes. Electroenceph Clin Neurophysiol 44(Suppl):55–75.

Schroeder CE, Mehta AD, Givre SJ (1998) A spatiotemporal profile of visual system activation revealed by current source density analysis in the awake macaque. Cereb Cortex 8:575–592.

Simson R, Vaughn HG Jr, Ritter W (1977) The scalp topography of potentials in auditory and visual discrimination tasks. Electroencephalogr Clin Neurophysiol 42:528–535.

Vaughan HG Jr, Arezzo JC (1988) The neural basis of event-related potentials. In: Human event-related potentials (Picton TW, ed.), vol. 3, pp. 45–94. New York: Elsevier Science Publishers.